EUROPEAN ORGANIZATION FOR NUCLEAR RESEARCH

CERN-EP-2001-042
June 21, 2001

Search for the decay $K_S \to \pi^0 e^+ e^-$

NA48 Collaboration

A. Lai, D. Marras
Dipartimento di Fisica dell'Università e Sezione dell'INFN di Cagliari, I-09100 Cagliari, Italy.

R. Batley, A. Bevan, R.S. Dosanjh, T.J. Gershon, G.E. Kalmus[1)], D.J. Munday, E. Olaiya, M.A. Parker, T.O. White, S.A. Wotton
Cavendish Laboratory, University of Cambridge, Cambridge, CB3 0HE, U.K.[2)]

G. Barr, G. Bocquet, A. Ceccucci, T. Cuhadar-Donszelmann, D. Cundy, N. Doble, V. Falaleev, L. Gatignon, A. Gonidec, B. Gorini, G. Govi, P. Grafström, W. Kubischta, A. Lacourt, M. Lenti[3)], A. Norton, S. Palestini, B. Panzer-Steindel, G. Tatishvili[4)], H. Taureg, M. Velasco, H. Wahl
CERN, CH-1211 Geneva 23, Switzerland.

C. Cheshkov, A. Gaponenko, P. Hristov[5)], V. Kekelidze, D. Madigojine, N. Molokanova, Yu. Potrebenikov, A. Tkatchev, A. Zinchenko
Joint Institute for Nuclear Research, Dubna, Russian Federation.

I. Knowles, C. Lazzeroni, V. Martin, R. Sacco, A. Walker
Department of Physics and Astronomy, University of Edinburgh, Edinburgh, EH9 3JZ, U.K.[6)]

M. Contalbrigo, P. Dalpiaz, J. Duclos, P.L. Frabetti, A. Gianoli, M. Martini, F. Petrucci, M. Savrié
Dipartimento di Fisica dell'Università e Sezione dell'INFN di Ferrara, I-44100 Ferrara, Italy.

A. Bizzeti[7)], M. Calvetti, G. Collazuol, G. Graziani, E. Iacopini
Dipartimento di Fisica dell'Università e Sezione dell'INFN di Firenze, I-50125 Firenze, Italy.

H.G. Becker, M. Eppard, H. Fox, K. Holtz, A. Kalter, K. Kleinknecht, U. Koch, L. Köpke, P.Lopes da Silva, P. Marouelli, I. Pellmann, A. Peters, B. Renk, S.A. Schmidt, V. Schönharting, Y. Schué, R. Wanke, A. Winhart, M. Wittgen
Institut für Physik, Universität Mainz, D-55099 Mainz, Germany[8)].

[1)] Based at Rutherford Appleton Laboratory, Chilton, Didcot, OX11 0QX, U.K.

[2)] Funded by the U.K. Particle Physics and Astronomy Research Council.

[3)] On leave from Sezione dell'INFN di Firenze, I-50125 Firenze, Italy.

[4)] On leave from Joint Institute for Nuclear Reaserch, Dubna, 141980, Russian Federation.

[5)] Present address: EP, CERN, CH-1211, Geneva 23, Switzerland.

[6)] Funded by the U.K. Particle Physics and Astronomy Research Council.

[7)] Dipartimento di Fisica dell'Università di Modena e Reggio Emilia, I-41100 Modena, Italy.

[8)] Funded by the German Federal Minister for Research and Technology (BMBF) under contract 7MZ18P(4)-TP2.

J.C. Chollet, L. Fayard, L. Iconomidou-Fayard, J. Ocariz, G. Unal, I. Wingerter-Seez
Laboratoire de l'Accélératur Linéaire, IN2P3-CNRS, Université de Paris-Sud, 91898 Orsay, France[9)].

G. Anzivino, P. Cenci, E. Imbergamo, P. Lubrano, A. Mestvirishvili, A. Nappi, M. Pepe, M. Piccini
Dipartimento di Fisica dell'Università e Sezione dell'INFN di Perugia, I-06100 Perugia, Italy.

R. Carosi, R. Casali, C. Cerri, M. Cirilli, F. Costantini, R. Fantechi, S. Giudici, I. Mannelli, G. Pierazzini, M. Sozzi
Dipartimento di Fisica dell'Università, Scuola Normale Superiore e Sezione INFN di Pisa, I-56100 Pisa, Italy.

J.B. Cheze, J. Cogan, M. De Beer, P. Debu, A. Formica, R. Granier de Cassagnac, E. Mazzucato, B. Peyaud, R. Turlay, B. Vallage
DSM/DAPNIA - CEA Saclay, F-91191 Gif-sur-Yvette Cedex, France.

M. Holder, A. Maier, M. Ziolkowski
Fachbereich Physik, Universität Siegen, D-57068 Siegen, Germany[10)].

R. Arcidiacono, C. Biino, N. Cartiglia, R. Guida, F. Marchetto, E. Menichetti, N. Pastrone
Dipartimento di Fisica Sperimentale dell'Università e Sezione dell'INFN di Torino, I-10125 Torino, Italy.

J. Nassalski, E. Rondio, M. Szleper, W. Wislicki, S. Wronka
Soltan Institute for Nuclear Studies, Laboratory for High Energy Physics, PL-00-681 Warsaw, Poland[11)].

H. Dibon, G. Fischer, M. Jeitler, M. Markytan, I. Mikulec, G. Neuhofer, M. Pernicka, A. Taurok, L. Widhalm
Österreichische Akademie der Wissenschaften, Institut für Hochenergiephysik, A-1050 Wien, Austria.

[9)] Funded by Institut National de Physique des Particules et de Physique Nucléaire (IN2P3), France.
[10)] Funded by the German Federal Minister for Research and Technology (BMBF) under contract 056SI74.
[11)] Supported by the KBN under contract SPUB-M/CERN/P03/DZ210/2000 and computing resources of the Interdisciplinary Center for Mathematical and Computational Modelling of the University of Warsaw.

Abstract

A search for the decay $K_S \to \pi^0 e^+ e^-$ has been made using the NA48 detector at the CERN SPS. Using data collected in 1999 during a 40-hour run with a high-intensity K_S beam, an upper limit for the branching fraction $B(K_S \to \pi^0 e^+ e^-) < 1.4 \times 10^{-7}$ at 90% confidence level has been obtained.

1 Introduction

Decays of K_L mesons into $\pi^0 l\bar{l}$ are of considerable interest due to their sensitivity to direct CP violation [1]. However, in $\pi^0 e^+ e^-$ decays both CP conserving and indirect CP violating amplitudes also contribute. The CP conserving contribution to this decay process can be obtained by measuring the low $m_{\gamma\gamma}$ component of the decay $K_L \to \pi^0\gamma\gamma$. The contribution to the branching ratio $B(K_L \to \pi^0 e^+ e^-)$ is $\approx 4 \times 10^{-12}$ [2]. The direct and indirect CP violating (CPV) contributions interfere, and their contribution to the branching ratio can be written as [3]:

$$B(K_L \to \pi^0 e^+ e^-)_{CPV} \times 10^{12} \simeq 15.3\, a_S^2 - 6.8\, a_S \frac{\mathrm{Im}(\lambda_t)}{10^{-4}} + 2.8 \left(\frac{\mathrm{Im}(\lambda_t)}{10^{-4}}\right)^2,$$

where $\lambda_t = V_{ts}^* V_{td}$ is the relevant combination of CKM matrix elements which describe the short distance CP violation. The parameter a_S describes the strength of the indirect CP violating component in the $K_L \to \pi^0 e^+ e^-$ decay, and is related to $B(K_S \to \pi^0 e^+ e^-)$ via [3]:

$$B(K_S \to \pi^0 e^+ e^-) = 5.2 \times 10^{-9}\, a_S^2.$$

According to dimensional analysis in chiral perturbation theory, $a_S \sim \mathcal{O}(1)$. The NA31 experiment obtained the upper bound $B(K_S \to \pi^0 e^+ e^-) < 1.1 \times 10^{-6}$ at 90% confidence level [4]. A more precise measurement of this mode is clearly important to place a bound on the indirect CP violating term in the K_L decay.

2 Experimental setup

The measurement was carried out using the NA48 detector at the CERN SPS, designed primarily to measure direct CP-violating effects in neutral kaon decays into two pions using simultaneous K_S and K_L beams. For the $K_S \to \pi^0 e^+ e^-$ search described here the K_L beam, normally present for the direct CP violation studies, was suppressed and the intensity of the K_S increased by a factor of ~ 200. The K_S beam was produced by 450 GeV/c protons, extracted from the accelerator during a 2.4 s spill every 14.4 s, and delivered to a 2 mm diameter, 400 mm long beryllium target at a production angle of 4.2 mrad in the vertical plane. The target was followed by a sweeping magnet and a set of collimators which defined a narrow beam of neutral particles, containing K^0 mesons and hyperons. The K_S beam angle was 0.6 mrad with respect to the symmetry axis along the beam pipe. The fiducial volume began about 6 m downstream of the K_S target and was contained in an evacuated steel cylinder about 89 m long and 2.4 m in diameter. The cylinder was closed at the downstream end by a polyimide (Kevlar) composite window and followed immediately by the main NA48 detector. A detailed description of the experimental layout can be found elsewhere [5].

The sub-detectors used in the investigation of $K_S \to \pi^0 e^+ e^-$ decays consists of:

a spectrometer composed of two drift chambers on either side of a dipole magnet; seven anti-counter rings of iron and plastic scintillator for vetoing photons outside the calorimeter acceptance; an electro-magnetic liquid-krypton calorimeter; a hadronic calorimeter and an arrangement of scintillators behind steel absorbers for detecting muons. The electro-magnetic calorimeter was used to measure energies, times and positions of electromagnetic showers. The momenta and positions of charged particles were measured using information from the drift chambers. The beginning of the decay region was defined by an "anti-K_S" counter (AKS), formed by scintillators[1)] placed in the K_S beam at the exit of the collimator. For this high-intensity run, the AKS was used as a charged particle veto counter.

The present analysis is based on data recorded during a 40-hour run in 1999 with an intensity of $\sim\ 6 \times 10^9$ protons per pulse on the K_S target.

The calibrated analogue sums of the electro-magnetic calorimeter cells were sent by the readout to the neutral trigger [6]. Horizontal (x) and vertical (y) projections of the calorimeter data were formed. These projections were then used to reconstruct the total energy E_0 deposited in the electro-magnetic calorimeter, the radial position C of the centre of energy of the event, the proper decay time τ (in units of the K_S lifetime τ_S measured from the AKS counter), and the number of energy peaks in x and y. Events were selected by the trigger if they satisfied the following conditions:

$$\max(n_X, n_Y) \leq 8; \quad E_0 > 50 \text{ GeV}; \quad C < 15 \text{ cm}; \quad \tau/\tau_S < 5$$

where n_X and n_Y are the number of peaks in x, y projections. In addition, an energy deposit of less than 10 GeV in the hadronic calorimeter and a minimum of one track reconstructed online were required.

About 4000 events per burst were selected by this trigger, representing 24% of the total trigger rate. About 80% of the data were collected with no downscaling, and the rest with a downscaling factor of two. This trigger was used to select $K_{\rm S} \to \pi^0\, e^+\, e^-$ and $K_{\rm S} \to \pi^0\, \pi^0_{\rm D} \to \gamma\gamma e^+ e^- \gamma$ decays, the latter being the normalisation channel.

A detector simulation based on Geant 3.21 [7] was used throughout this analysis.

3 Data analysis

3.1 Event selection

To select $K_{\rm S} \to \pi^0\, e^+\, e^-$ candidates, all events satisfying the trigger and with at least four electro-magnetic clusters, and two tracks making a vertex were further analysed. For each event, all combinations of four clusters were considered. The following selection criteria were applied to each combination:

1) the sum of the cluster energies had to be greater than 60 GeV and less than 190 GeV;
2) the energy of each of cluster had to be greater than 3 GeV and less than 100 GeV, high enough to guarantee a good energy resolution and well above the detector noise of 90 MeV per cluster;
3) each cluster had to be at least 6 cm from any other cluster in the event;
4) to ensure negligible energy loss, each cluster had to be more than 15 cm from the centre of the beam pipe and more than 10 cm from the outer edge of the calorimeter; the distance of each cluster from any calorimeter dead cells had to exceed 2 cm;

[1)] The AKS scintillators are normally preceded by an iridium crystal that was removed during this high-intensity run to reduce the rate in the detector.

5) for groups of four clusters satisfying these requirements, the event time was computed from the average time of the selected clusters; all clusters had to be within ± 3 ns of the event time.

Furthermore, the following conditions were imposed on the events:

6) as a test for any missed energy in the event, a function defined as

$$cog = \frac{\sqrt{(\sum_i E_i x_i)^2 + (\sum_i E_i y_i)^2}}{\sum_i E_i}$$

was constructed (E_i, x_i and y_i are the energy and position of the i-th cluster). Only events where the value of *cog* was less than 10 cm were kept. Typically *cog* is less than 5 cm for $2\pi^0$ events if no energy is lost;

7) to minimise the effect of background in time with the event, it was required that no other cluster (i.e. not belonging to the combination considered) with energy greater than 1.5 GeV was within 3 ns of the event time [5];

8) electron candidates were identified by requiring the cluster centres in the electromagnetic calorimeter to be within 1.5 cm of the expected position based on extrapolation of each track from the drift chambers;

9) for charged tracks, the ratio E/p of the energy measured in the calorimeter and the momentum measured by the drift chambers was required to be between 0.9 and 1.1 for electron identification;

10) to maintain the highest detector efficiency, it was required that events did not have an overflow condition resetting the front-end readout buffers within ± 312 ns of the trigger time;

11) the momentum of each electron candidate had to be greater than 4 GeV/c;

12) the electron tracks were required to be separated by at least 2 cm in the first drift chamber. This criterion was effective in rejecting events in which a photon converted in material before the magnet;

13) the track time was calculated from drift chamber information; to further reject accidental activity in the detector, the time separation between any pair of tracks, and between any track and its associated cluster in the calorimeter had to be less than 10 ns;

14) to suppress decays into charged hadrons, the total deposited energy in the hadron calorimeter was required to be less than 6 GeV;

15) events, with hits in the muon detector consistent with the extrapolation of tracks from the drift chambers, were rejected if the muon detector time was within 4 ns of the event time;

16) since the beginning of the fiducial volume was defined by the position of the downstream scintillator of the AKS, an anti-coincidence between the event time and the AKS time was required;

17) Among all the good combinations, the one with the closest mass to the nominal π^0 mass and then the closest mass to the nominal K_S mass was chosen.
This condition was accomplished in the following way. For each combination of clusters and vertices that satisfied the requirements described above, π^0 and K^0 masses were computed. Candidate π^0s were formed from the pair of clusters in the electro-magnetic calorimeter with no associated tracks, taking the longitudinal position of the 'neutral vertex', $z_{neutral}$, as the kaon decay point. The $z_{neutral}$ was defined using the kaon mass constraint as

$$z_{neutral} = z_{\rm LKr} - \frac{\sqrt{\sum_{i,j(i>j)} E_i E_j [(x_i - x_j)^2 + (y_i - y_j)^2]}}{m_{\rm K}}$$

where $z_{\rm LKr}$ is the z coordinate of the calorimeter front face with respect to the target; $E_{i(j)}$, $x_{i(j)}$ and $y_{i(j)}$ are the energy and positions of the $i(j)$-th cluster, and $m_{\rm K}$ is the kaon mass. For electron tracks, the extrapolation from the drift chamber before the magnet to the calorimeter surface was used in this calculation instead of the actual cluster positions. The resolution of the neutral vertex reconstruction was determined from simulation and is about 44 cm.

Kaon candidates were formed from the clusters associated with the neutral pion and the clusters associated with the electron tracks, assuming the longitudinal position of the 'charged vertex', $z_{charged}$, as the decay point. The x and y coordinates of the charged vertex are found by extrapolating the positions of the two tracks before the magnet to the position of $z_{neutral}$. The average of the two measurements is taken as the x-y vertex position. The z position of the charged vertex can be calculated using the constraint that the kaon decay should lie on the line that goes from the target to the point (x_{cog}, y_{cog}), where $x_{cog} = (\sum_i E_i x_i)/\sum_i E_i$ and $y_{cog} = (\sum_i E_i y_i)/\sum_i E_i$ (E_i, x_i and y_i are the energy and positions of the i-th cluster). For each track, the closest distance of approach between this line and the track can be found, giving two measurements of the z position which are then averaged to give $z_{charged}$;

18) the end of the fiducial volume was defined as 4 τ_s. The proper time of the decay, τ, was determined from the energy and the longitudinal position of the 'neutral vertex' $z_{neutral}$.

3.2 Background rejection

To reject background, further requirements were imposed. The invariant $\gamma\gamma$ mass was required to be within 3 MeV/c^2 of the nominal π^0 mass, corresponding to about 2 standard deviations of the π^0 mass resolution. The invariant mass of $\pi^0 e^+ e^-$ candidates was required to be within 10 MeV/c^2 of the nominal K^0 mass, equivalent to about 3 standard deviations of the K^0 mass resolution.

A potentially severe background mode is the decay $K_{\rm S} \to \pi^0_{\rm D}\,\pi^0_{\rm D}$, where both π^0s undergo Dalitz decays ($\pi^0 \to e^+ e^- \gamma$) and one electron and one positron from different π^0s are lost. To reject events from this decay, the invariant masses $m_{e^+\gamma_1}$, $m_{e^-\gamma_2}$ and $m_{e^+\gamma_2}$, $m_{e^-\gamma_1}$ of electron-photon pairs were calculated for each event using the neutral vertex. For each of the four mass combinations it was required that at least one combination had $|m_{e\gamma} - m_{\pi^0}| > 30$ MeV/c^2. This cut rejected the bulk of this background, while retaining virtually full acceptance for the signal. The distribution of $m_{e^+\gamma_1}$ versus $m_{e^-\gamma_2}$ for $K_{\rm S} \to \pi^0\, e^+\, e^-$ and $K_{\rm S} \to \pi^0_{\rm D}\,\pi^0_{\rm D}$ decays is shown in Fig. 1. Using a simulation based on 7×10^5 $K_{\rm S} \to \pi^0_{\rm D}\,\pi^0_{\rm D}$ events it was calculated that less than 0.01 $K_{\rm S} \to \pi^0_{\rm D}\,\pi^0_{\rm D}$ events were expected to fulfil the above requirements and be misidentified as signal candidates in our data sample.

The main background to $K_{\rm S} \to \pi^0\, e^+\, e^-$ decays was found to be $K_{\rm S} \to \pi^0\,\pi^0_{\rm D}$ decays with one lost photon. The invariant mass of the electrons cannot exceed $m_{\pi^0} = 135\,{\rm MeV}/c^2$. However, interactions in the detector such as bremsstrahlung and pair production, and the misreconstruction of the two tracks partially result in some of these $K_{\rm S} \to \pi^0\,\pi^0_{\rm D}$ events being reconstructed with $m_{e^+e^-}$ above the kinematic limit.

To reject this background, a sample of 3×10^7 $K_{\rm S} \to \pi^0\,\pi^0_{\rm D}$ decays was simulated.

No event with m_{ee} greater than 165 MeV/c^2 was found, and this cut was applied to our data. Less than 0.15 events were then expected to remain in our data sample.

Other $K_{\rm S}$ and $K_{\rm L}$ decays which might fake $K_{\rm S} \to \pi^0\, e^+\, e^-$ decays have also been considered and simulated. In particular, the contribution to the background from the decays $K_{\rm L,S} \to e^+e^-\gamma\gamma$, where the invariant $\gamma\gamma$ mass falls into the π^0 mass window, and from the decays $K_{\rm S} \to \pi^0_{\rm D}\, \pi^0_{\rm DD}$, where π^0 undergo double Dalitz decay ($\pi^0_{\rm DD} \to e^+e^-e^+e^-$) with one lost electron and one lost positron, were found to be negligible without the addition of any further cuts.

3.3 $K_{\rm S} \to \pi^0\, e^+\, e^-$ acceptance evaluation

For the calculation of the $K_{\rm S} \to \pi^0\, e^+\, e^-$ acceptance, the matrix element for this decay was derived using Chiral Perturbation Theory [3]:

$$A[K(k) \to \pi(p) e^+(p_+) e^-(p_-)] = \frac{-e^2}{{m_{\rm K}}^2 (4\pi)^2} W(z)(k+p)^\mu \bar{u}_l(p_-)\gamma_\mu v_l(p_+)$$

where k, p, p_+ and p_- are the four-momenta of the kaon, pion, positron and electron respectively; $m_{\rm K}$ is the kaon mass; $W(z)$ is the electro-magnetic transition form factor, with $z = (k-p)^2/{m_{\rm K}}^2$. As a consequence of gauge invariance, the form factor vanishes to lowest order in the low-energy expansion in z and therefore can be represented as a polynomial. For K_S decays, the form factor $W(z)$ can be approximated to $W(z) \simeq 1 + z/{r_{\rm V}}^2$ where ${r_{\rm V}}^2 = {m_{\rm V}}^2/{m_{\rm K}}^2 \simeq 2.5$, $m_{\rm V}$ being the vector meson mass in the Vector Meson Dominance model [3]. The radiative corrections for final state interactions have been taken into account [8].

The geometrical acceptance for $K_{\rm S} \to \pi^0\, e^+\, e^-$ decays has been calculated to be 31%, while the overall acceptance after all requirements to be 7.6%. The sensitivity to the exact form of $W(z)$ was estimated by varying $1/{r_{\rm V}}^2$ between 0.2 and 0.6 [2]; the overall acceptance changed from to 7.2% to 8.1%.

The trigger efficiencies for accepted $K_{\rm S} \to \pi^0\, e^+\, e^-$ and $K_{\rm S} \to \pi^0\, \pi^0_{\rm D}$ decays have been calculated from simulation to be 98.3% for $K_{\rm S} \to \pi^0\, e^+\, e^-$ and 99.7% for $K_{\rm S} \to \pi^0\, \pi^0_{\rm D}$. For the latter decay, the efficiency has also been directly measured from data and found to be fully consistent with the estimates. Taking into account the trigger efficiency of 98.3%, the overall acceptance for $K_{\rm S} \to \pi^0\, e^+\, e^-$ decays was reduced from 7.6% to 7.5%.

Table 1 shows the acceptances, with the number of events and the expected background at different stages of the selection. The distributions of generated m_{ee} and the relative acceptance for $K_{\rm S} \to \pi^0\, e^+\, e^-$ decays are shown in Fig. 2. The distributions of reconstructed m_{ee} after $m_{\rm K}$ cut and after $m_{e\gamma}$ cut are shown in Fig. 3, for data and simulation.

After applying all requirements, no $K_{\rm S} \to \pi^0\, e^+\, e^-$ candidate remained in the data sample.

4 Normalisation

In order to determine the K_S flux in the beam, the decay $K_{\rm S} \to \pi^0\, \pi^0_{\rm D}$ was used for normalisation because of its similar topology to the signal. Since both the signal and the normalisation modes consist of 2-track events, uncertainties due to tracking tend to cancel in the ratio of acceptances. Selection criteria identical to those used in the signal mode were applied, with the following exceptions: events with at least five clusters, instead of four, were selected; no cut was applied to the invariant mass of the e^+e^- pair and of the

Requirement	$\alpha(K_S \to \pi^0 e^+ e^-)$ (%)	Events from data	Expect. Bkg from MC
$\lvert m_{ee\gamma\gamma} - m_K \rvert < 10$ MeV/c^2	15.9	472	446
$\tau < 4\tau_s$	15.7	457	427
$\lvert m_{\gamma\gamma} - m_{\pi^0} \rvert < 3$ MeV/c^2	15.3	23	23
$\lvert m_{e1\gamma1}, m_{e2\gamma2} - m_{\pi^0} \rvert > 30$ MeV/c^2	14.6	23	23
$m_{ee} > 165$ MeV/c^2	7.6	0	<0.15

Table 1: Summary of requirements applied. The acceptances α are evaluated from simulated $K_S \to \pi^0 e^+ e^-$ events. The number of events is from the data. The expected background takes into account the contribution from the relevant sources, such as $K_S \to \pi^0 \pi^0_D$, $K_S \to \pi^0_D \pi^0_D$ and $K_S \to \pi^0 \pi^0$, using the evaluated acceptances for these channels and the estimated kaon flux. The background estimate is entirely limited by simulation statistics.

$e\gamma$ pair. To select π^0 candidates the neutral vertex was assumed to be the decay point; the neutral vertex resolution for these events varied in the range of 42-46 cm depending on the kaon energy.

A χ^2-like variable, $R_{\rm ellipse}$, was defined as follows:

$$R_{\rm ellipse} = \frac{1}{9}\left[\left(\frac{(m_{\gamma\gamma}+m_{ee\gamma})/2 - m_{\pi^0}}{\sigma_+}\right)^2 + \left(\frac{(m_{\gamma\gamma}-m_{ee\gamma})/2}{\sigma_-}\right)^2\right],$$

where $m_{\gamma\gamma}$ and $m_{ee\gamma}$ are the invariant masses of the $\gamma\gamma$ and $ee\gamma$ combinations; $\sigma_{+,-}$ are the resolutions for the mass sum and difference, measured from the data and parametrised as a function of the lowest photon energy. This χ^2-like variable tests the agreement between the invariant masses of possible photon pairs and the π^0 mass. Although $m_{\gamma\gamma}$ and $m_{ee\gamma}$ are correlated because of the constraint on m_K in the $z_{neutral}$ definition, $m_{\gamma\gamma} + m_{ee\gamma}$ and $m_{\gamma\gamma} - m_{ee\gamma}$ are, to a good approximation, uncorrelated. The requirement $R_{\rm ellipse} < 3$, corresponding to about $5\sigma_{\pi^0}$, was applied to reject the events where the non-Gaussian tails in energy resolution became more relevant.

The resolution of the invariant masses $m_{\gamma\gamma}$ and $m_{ee\gamma}$ was measured to be $\sim$ 1 MeV/c^2 for both data and simulation.

Simulation studies showed that about 370 of the reconstructed $K_S \to \pi^0 \pi^0_D$ candidates came from K_S decaying before the AKS counter; these decays were not detected because of the veto dead-time, measured experimentally to be about 10%. Similarly, about 1340 $K_S \to \pi^0 \pi^0$ decays where a photon converted in the AKS during veto dead-time were reconstructed as $K_S \to \pi^0 \pi^0_D$ decays.

Another possible source of background came from $K_S \to \pi^0 \pi^0$ decays where a photon converted at the end of the AKS counter. Conversions occurring in the last $\sim$ 0.75 mm of the downstream scintillator gave signals below the detection threshold and such conversions were therefore not vetoed. The number of such decays was estimated to give a negligible contribution to the background.

The background from the decay $K_S \to \pi^0_D \pi^0_D$ with one bremsstrahlung photon, and from the decay $K_S \to \pi^0_D \pi^0_{DD}$ with two lost electrons, were studied using simulation and found to be negligible.

Other possible sources of background were considered, in particular those from K_L decays. K_S and K_L mesons were produced in the target with the ratio 1:1, but the large K_L lifetime considerably reduced the background from K_L decays. From simulation, a

rejection factor of 10^6 for $K_L \to \pi^+\pi^-\pi^0$ and a rejection factor of 0.5×10^6 for $K_L \to \pi^0\pi^0\pi^0$ were obtained, thus the background from these channels was also negligible.

The selection acceptance was 4.4%, determined from simulation where radiative corrections [8] and trigger inefficiency were taken into account. Using the cuts described above, 77310 $K_S \to \pi^0\,\pi^0_D$ decays remained after background subtraction.

Using the branching ratio $B(K_S \to \pi^0\,\pi^0_D) = (7.43 \pm 0.19) \times 10^{-3}$ [9], the selected $K_S \to \pi^0\,\pi^0_D$ decays corresponded to a flux of K_S in the fiducial volume of 2.36×10^8. The total K_S flux was calculated to be 2.80×10^8 after taking into account the downscaling in the trigger for part of the data.

The distributions of m_{ee} and $R_{\rm ellipse}$ for $K_S \to \pi^0\,\pi^0_D$ from data and from simulation are shown in Fig. 4. These distributions have been corrected to take into account all background sources.

5 Systematic uncertainties

The following sources of systematic uncertainties were considered:

1) variations of the selection cuts produced a change in the calculated flux of 1.5%;
2) the AKS active time varied from 92% to 88% depending on intensity; because it affected only the background subtraction, this variation produced a systematic uncertainty of less than 1%;
3) varying the cut-off applied to the energy of the photon emitted in radiative corrections from 10 MeV to 5 MeV produced a difference of less than 1% in the ratio between the acceptances of signal and normalisation channel; not using the radiative corrections produced a variation in the single acceptances of about 10% but the variation in their ratio was less than 2%;
4) varying the coefficient of the linear expansion of the $K_S \to \pi^0\,e^+\,e^-$ form factor by 0.4 ± 0.2 corresponded to a change of $\pm 6\%$ in the overall acceptance;
5) the uncertainty of 2.6% on the Dalitz branching fraction caused a systematic uncertainty of the same amount.

Other possible sources of systematic uncertainty were studied but found to have a negligible impact on the result. The loss due to the cut on events accidentally in-time has been evaluated to be about 1.5%, but is symmetric to first order between signal and normalisation channel, and the size of the effect can therefore be considered negligible. The difference in the trigger acceptance for Dalitz decays as measured from real data and from simulated events also caused a negligible effect.

The overall uncertainty has been estimated to be 7% and has a negligible effect on the result [10].

6 Result and Conclusion

No event satisfying all the $K_S \to \pi^0\,e^+\,e^-$ requirements was seen. The signal acceptance was calculated to be $\alpha_{\pi^0 e^+ e^-} = 7.5\%$, assuming the matrix element $W(z) \simeq 1 + z/{r_V}^2 = 1 + z/2.5$ as described above [3]. Using the K_S flux of 2.36×10^8, and a value $N_{\pi^0 e^+ e^-} = 2.44$ for the number of events, corresponding to a confidence level of 90% when no events are seen [9], an upper limit was found for the branching ratio of the decay $K_S \to \pi^0\,e^+\,e^-$:

$$B(K_S \to \pi^0\,e^+\,e^-) \;=\; \frac{N_{\pi^0 e^+ e^-}}{(K_S\ \text{Flux})\ \alpha_{\pi^0 e^+ e^-}} \;<\; 1.4 \;\times\; 10^{-7}$$

This limit is an order of magnitude below the previously published value [4], but does not yet constrain usefully the parameter a_S. This result is consistent with the one that can be derived from the recently published limit $\mathrm{B}(K_\mathrm{L} \to \pi^0 e^+ e^-) < 5.1 \times 10^{-10}$ [11].

Acknowledgements

It is a pleasure to thank the technical staff of the participating laboratories, universities and affiliated computing centres for their efforts in the construction of the NA48 apparatus, in the operation of the experiment, and in the processing of the data.

References

[1] G. D'Ambrosio and G. Isidori, Int.J.Mod.Phys. **A13**, 1 (1998)
[2] G. Isidori, hep-ph/9908399 (1999).
[3] G. D'Ambrosio, G. Ecker, G. Isidori and J. Portoles, JHEP 08(1998)004.
[4] G. Barr *et al.*, (NA31 Collaboration), Phys. Lett. **B304**, 381 (1993).
[5] V. Fanti *et al.*, (NA48 Collaboration), Phys. Lett. **B465**, 335 (1999).
V. Fanti *et al.*, 'The beam and detector for a precision CP violation experiment NA48', in preparation.
[6] B. Gorini *et al.*, IEEE Trans. Nucl. Sci. **45**, 1771 (1998).
[7] GEANT Detector Description and Simulation Tool, CERN Program Library Long Writeup W5013 (1994).
[8] E. Barberio and Z. Was, Comput. Phys. Commun. **79**, 291 (1994).
E. Barberio, B. Van Eijk and Z. Was, CERN-TH-5857/90.
[9] D. E. Groom *et al.*, Eur. Phys. J. **C15** (2000).
[10] R. D. Cousins and V. L. Highland, Nucl. Instr. Meth. **A320**, 331 (1992).
[11] A. Alavi-Harati *et al.* (KTeV Collaboration), Phys. Rev. Lett. **86**, 397 (2001).

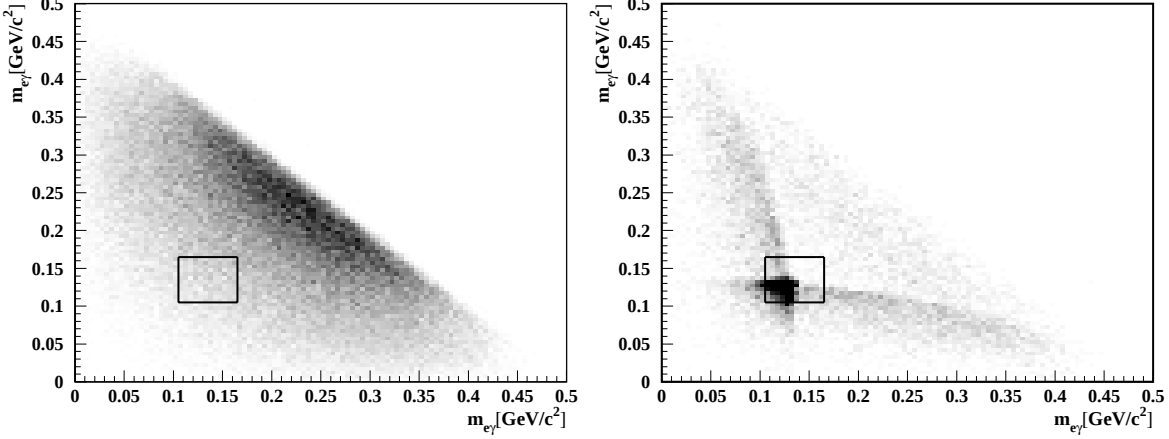

Figure 1: Invariant mass distribution of one $e\gamma$ pair versus the invariant mass of the other pair. Shown are $K_{\rm S} \to \pi^0\, e^+\, e^-$ simulation (left), and $K_{\rm S} \to \pi^0_{\rm D}\, \pi^0_{\rm D}$ simulation (right). The box represents the veto cut around the pion mass.

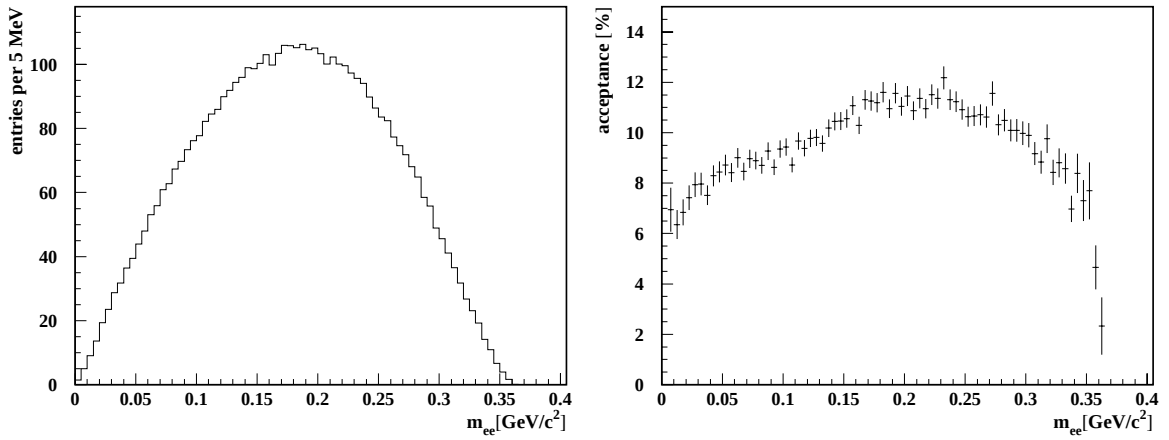

Figure 2: Distribution of generated invariant mass of the e^+e^- pair for simulated $K_{\rm S} \to \pi^0\, e^+\, e^-$ events (left), and acceptance as a function of m_{ee} (right). The absolute normalisation in (left) is arbitrary.

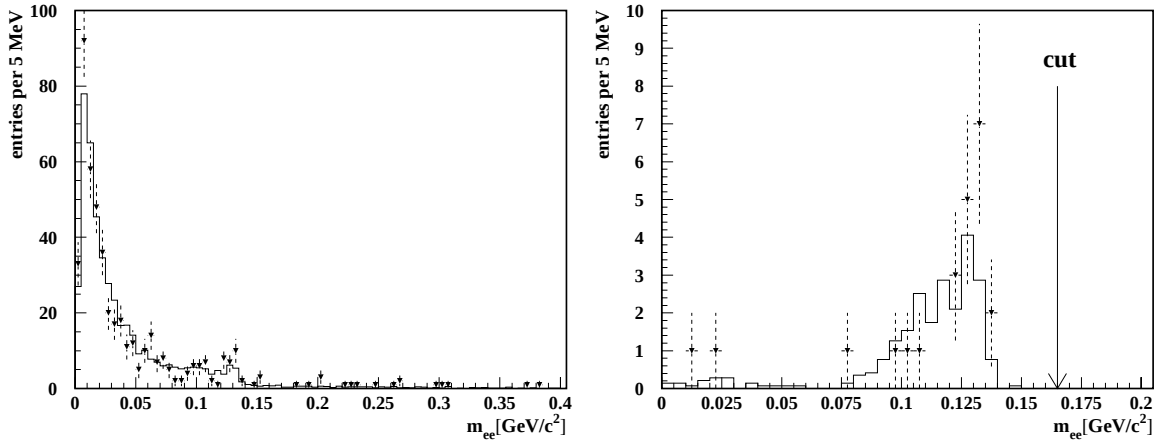

Figure 3: Reconstructed invariant mass distribution of the e^+e^- pair after $m_{\rm K}$ cut (left), and after $m_{e\gamma}$ cut (right), for simulation (solid line) and data (triangles) selected as $K_{\rm S} \to \pi^0\, e^+\, e^-$. No events are left above 0.15 MeV/c^2.

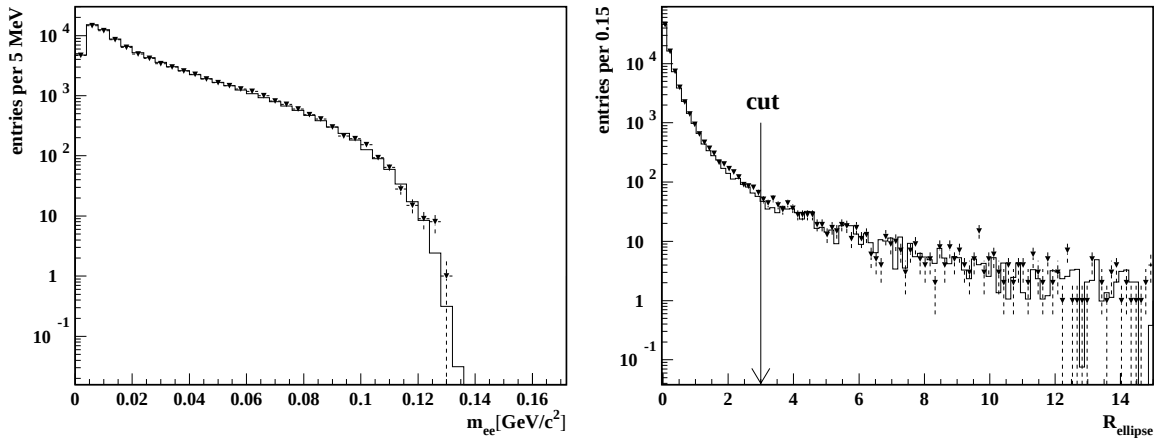

Figure 4: Distribution of reconstructed invariant mass of the e^+e^- pair (left), and $R_{\rm ellipse}$ (right), for simulation (solid line) and for data (triangles) selected as $K_{\rm S} \to \pi^0\, \pi^0_{\rm D}$. The simulation curves have been normalised to the data. The cut applied is shown.